Cryobiology 75 (2017) 7–14

Contents lists available at ScienceDirect

Cryobiology

journal homepage: www.elsevier.com/locate/ycryo

Cryopreservation and multipotential characteristics evaluation of a novel type of mesenchymal stem cells derived from Small Tailed Han Sheep fetal lung tissue

Caiyun Ma [a, 1], Changqing Liu [a, b, 1], Xiangchen Li [a], Taofeng Lu [c], Chunyu Bai [a], Yanan Fan [a], Weijun Guan [a, *], Yu Guo [a, b, **]

[a] Institute of Beijing Animal Science and Veterinary, Chinese Academy of Agricultural Science, Beijing, 100193, China
[b] Department of Life Science, Department of laboratory medicine, Bengbu Medical College, Bengbu, 233030, China
[c] Harbin Veterinary Research Institute, Chinese Academy of Agricultural Sciences, Harbin, 150001, China

ARTICLE INFO

Article history:
Received 18 November 2016
Accepted 6 March 2017
Available online 8 March 2017

Keywords:
Fetal Small Tailed Han Sheep
Lung mesenchymal stem cells
Cryopreservation
Differentiation potential
Regenerative therapies

ABSTRACT

Lung mesenchymal stem cells (L-MSCs) characterized by plasticity, reduced relative immune privilege and high anti-fibrosis characteristics play the crucial role in lung tissue regenerative processes. However, up to date, the multi-differentiation potentials and application values of L-MSCs are still uncertain. In the current study, the Small Tailed Han Sheep embryo L-MSCs line from 12 samples, stocking 124 cryogenically-preserved vials, was successfully established by using primary culture and cell cryopreservation techniques. Isolated L-MSCs were morphologically consistent with fibroblasts, could be passaged for at least 18 passages and more than 91.8% of cells were diploid (2n = 54) analyze by G-banding. The majority of cells were in the G0/G1 phase (70.5–91.2%), and the growth curves were all typically sigmoidal. Moreover, L-MSCs were found to express pluripotent genes Oct4, Nanog and MSCs-associated genes β-integrin, CD29, CD44, CD71, CD73 and CD90, while the expressions of hematopoietic cell markers CD34 and CD45 were negative. In addtion, the L-MSCs could be differentiated into cells of three layers with induction medium *in vitro*, which confirmed their multilineage differentiation potential. The secretion of urea and ALB showed the differentiated hepatocytes still possessed the detoxification function. These results indicated that the isolated L-MSCs displayed typical characteristics of mesenchymal stem cells and that the culture conditions were suitable for their maintenance of stemness and their proliferation *in vitro*.

1. Introduction

Despite these beneficial features of embryonic stem cells and induced pluripotent stem cells (iPSCs), their clinical applications have significant disadvantages such as various ethical issues, reprogramming inconsistency and their remarkable plasticity could lead to tumorigenesis [3,11]. Currently, mesenchymal stem cells (MSCs) are deeply studied and considered as the most valuable cell sources for regenerative medicine because of their capability for self-renewal and differentiation potential [16]. Previous reports have shown the presence of MSCs in various tissues, such as blood, bone marrow, liver, lung, pangreas and spleen [5], and even in extraembryonic tissues [20]. Recently, some research showed that multipotent cells from non-controversial fetal tissues possessed biological characteristics like bone marrow MSCs [6]. Moreover, these cells have been demonstrated with greater proliferation and differentiation capacity than adult's MSCs, which will give greater potency to treat incurable or degenerative diseases [22].

Lung diseases have become severe diseases in the whole world. Moreover, no effective clinical therapies to cure lung disease are available till now [19]. Fortunately, some recent preclinical studies have evidenced the L-MSCs can participate in the development of lung tissue and increase the proliferative capacity of the

* Corresponding author. Institute of Animal Science, Chinese Academy of Agricultural Science, 2 Yuanmingyuan West Road, Beijing 100193, China.
** Corresponding author. Department of laboratory medicine, 2600 Donghai Road, Bengbu Medical College, Bengbu 233030, China.
E-mail addresses: wjguan86@iascaas.net.cn (W. Guan), ily0720@126.com (Y. Guo).
[1] Dr. Caiyun Ma and Changqing Liu contributed equally to this work and shared the first authorship.

http://dx.doi.org/10.1016/j.cryobiol.2017.03.003
0011-2240/

bronchioalveolar stem cell, acting as attractive candidates to treat many lung diseases, specifically for anti-fibrotic properties and immunosuppressive properties [8,16].

The vast majority of existing studies associated with stem cells transplantation mainly focused on humans, mice, rabbits, but little research paper had been done on sheep. Currently, there are numerous pivotal problems remain unresolved for L-MSCs, such as efficient isolated method, immunoregulation, application potential and specific surface markers. In the current study, we aimed to isolate L-MSCs from lung tissue of fetal sheep, and to detect their significant pluripotent features, in terms of phenotype, proliferative capacity, specific markers and differentiation potential, in order to establish a larger experimental animal model for regenerative research.

2. Materials and methods

2.1. Cell isolation and in vitro culture of L-MSCs of fetal sheep

Small Tailed Han Sheep (45-day-old embryos from 12 individual, 6 male and 6 female) were provided by the Chinese Academy of Agriculture Sciences, China. And, the use of animals and all experimental procedures were conducted in accordance with the guidelines of Ethics Committee of Beijing. The pulmonary parenchyma were diced and incubated with 0.2% collagenase type II at 37 °C for 40–50 min. And then, the suspension was filtered through a 200 μm mesh filter and centrifuged at 1200 rpm for 8 min. Subsequently, cell pellets were resuspended in complete medium (H-DMEM, 10%FBS+10 ng/mL bFGF) at 1×10^5 cells/mL, and incubated in a humidified incubator at 37 °C with 5% CO_2. The adherent cells were digested with 0.25% trypsin to further expansion at 80%–90% confluency. Then, cell suspension ($1–3 \times 10^6$ cells/mL) was dispensed into 1.8 mL sterile cryogenic vials and transferred to liquid nitrogen for long term storage after programmed freezing by a CyroMed freezer (Thermo Scientific) [7].

2.2. Colony-forming cell assay, cell population dynamics and G-banding assay

Cells from passage 5, 10 and 18 were seeded in 24-well microplates and cultured for 7–10 days for CFU assay. Colony-forming units were stained by Giemsa and counted under the microscope. Colonies aggregating at least 50 cells were counted and the cloning efficiency was calculated as: CFU numbers/starting cell number × 100%. The cell proliferation ability was assessed by immunofluorescence using monoclonal antibody anti-BrdU (1:200, Santa Cruz, CA). The growth curves and cumulative population doubling times (PDTs) were calculated [1]. Metaphase chromosomes spreads were prepared, fixed and stained by Giemsa.

2.3. Immunofluorescence and flow cytometry analysis for surface antigen marker

L-MSCs were fixed with 4% paraformaldehyde (PFA) and permeabilized with PBS containing 0.1%Triton X-100 for 20 min, and then blocking with 10% normal goat serum for 30 min. The following primary antibodies were used to incubate with the cells overnight at 4 °C, mouse anti-CD29, rat anti-CD44, mouse anti-Map2 (1:200; Abcam, Cambridge, MA, USA), rabbit anti-CD71, rabbit anti-CD73, rabbit anti-CD90, rabbit anti-Nestin (1:200; Bioss, Beijing, China). Subsequently, the cells incubated with FITC- or TRITC- conjugated secondary antibody (1:100; Santa Cruz, CA, USA) at 37 °C for 1 h. Fluorescence signals were detected under confocal microscopy (Nikon TE-2000-E, Tokyo, Japan) and quantified by video densitometric analysis using image software.

L-MSCs in logarithmic phase were harvested and stained with Propidium Iodide (PI, 0.05 mg/ml) for cell cycle distributions analysis by flow cytometry (Cytomics FC 500, Beckman Coulter, USA) [10]. The proportions of apoptotic cells were evaluated using an Annexin V/FITC staining kit (Beyotime, Jiangsu, China). Expression of cell surface markers were detected by incubating with fluorescence-conjugated mouse anti-CD29, rat anti-CD44, rabbit anti-CD71, rabbit anti-CD73, rabbit anti-CD90 monoclonal antibodies using flow cytometry.

2.4. Gene expression analysis

The total RNAs were extracted from L-MSCs or differentiation induced cells using Trizol reagent (Invitrogen, Carlsbad, USA) according to the manufacturer's protocols. RNA concentration and purity was further detected at an optical density ratio of 260/280 and Agilent 2100 Bioanalyzer. The relative quantitative real-time PCR was carried out with SYBR® Premix Ex Taq™ kit (TaKaRa) on an Applied Biosystems QuantStudio™6 Flex thermocycler [21], and GAPDH was used as an internal control. The primers used in PCR reactions were indicated in Table S1.

2.5. In vitro differentiation into adipocytes, osteoblasts and chondrocytes

Adipogenic differentiation of L-MSCs was incubated in H-DMEM supplemented with 10% FBS, 1 mM dexamethasone, 0.5 mM IBMX, 10 μg/mL insulin and 60 μM indomethacin for 21 days, as previously reported [14]. Adipogenesis was assessed by Oil red staining and adipocytes specific genes detection. For osteoblastic differentiation, the L-MSCs were cultured with osteogenic inducers including H-DMEM consisted of 10% FBS, 0.5 mM dexamethasone, 10 mM β-glycerophosphate and 50 μg/mL vitamin C [2]. The differentiation potential of L-MSCs to osteoblast was assessed according to the accumulated calcium node stained by Alizarin Red and osteogenic specific genes detection. For chondrogenic differentiation, the L-MSCs were cultured in chondrogenic medium consisting of 5% FBS, 1% ITS, 50 μg/mL L-proline, 0.1 μM dexamethasone, 0.9 mM sodium pyruvate, 50 μg/mL vitamin C and 10 ng/mL TGF-β3, and chondrogenesis was assessed by Toluidine Blue, Alcian Blue staining and chondrogenic specific genes detection.

2.6. β-cell, hepatocytes and neurocyte differentiation

Insulin-producing β-like cells was confirmed by the formation of islet-like clusters, dithizone (DTZ) staining, immunocytochemical detection for insulin (1:200, Bioss). Hepatic differentiation of L-MSCs was induced for 14 days according to the published protocols with minor improvements [12], and the induced cells were stained by Periodic Acid-Schiff (PAS) glucogen staining and liver-associated genes detection. The concentrations of urea and albumin were assayed in supernatants using enzyme-linked immunosorbent assay (ELISA). For neuronal differentiation, L-MSCs were seeded in six-well plates and treated with H-DMEM supplemented with 10% FBS, initially supplemented with 2% B27 Supplement, 2 mM L-glutamine, 40 ng/mL bFGF, 20 ng/mL EGF for 6 days. After that, 1% N_2 Supplement, 10 ng/mL Glial-Derived Neurotrophic Factor (GDNF) and 50 μg/mL vitamin C were added [4]. After induced for 14 days, the neural-specific markers were detected by immunocytochemical staining and RT-PCR.

3. Results

3.1. Morphology, G-Banding and phenotypes of cultured L-MSCs

Primary cells consisted of heterogeneous population with round-shape/flattened irregular, and spindle cells. Relatively homogenous population of typical fibroblast-like cells was obtained after subsequent subculture 3–4 passages (Fig. 1A). No significant morphological differences were identified during the following serial passage, and the undifferentiated cell states were stable. The viabilities before cryo-preservation and after recovery of L-MSCs detected by Trypan Blue staining were 96.5% ± 1.42% and 93.8% ± 2.54%, respectively. Merely, the highest number of passages achievable for L-MSCs was 18, after that most cells would exhibit representative signs of senescent, characterized by vacuoles and karyopyknosis (Fig. 1A). Chromosome G-Banding showed that the frequencies of cells from P5, P10, P18 with 2n = 54 were 95.2%, 93.6% and 91.8%, respectively. These results indicated that they were not cross-contamination by other cell types, and supported the L-MSCs cell line was reproducibly diploid (Fig. 1D).

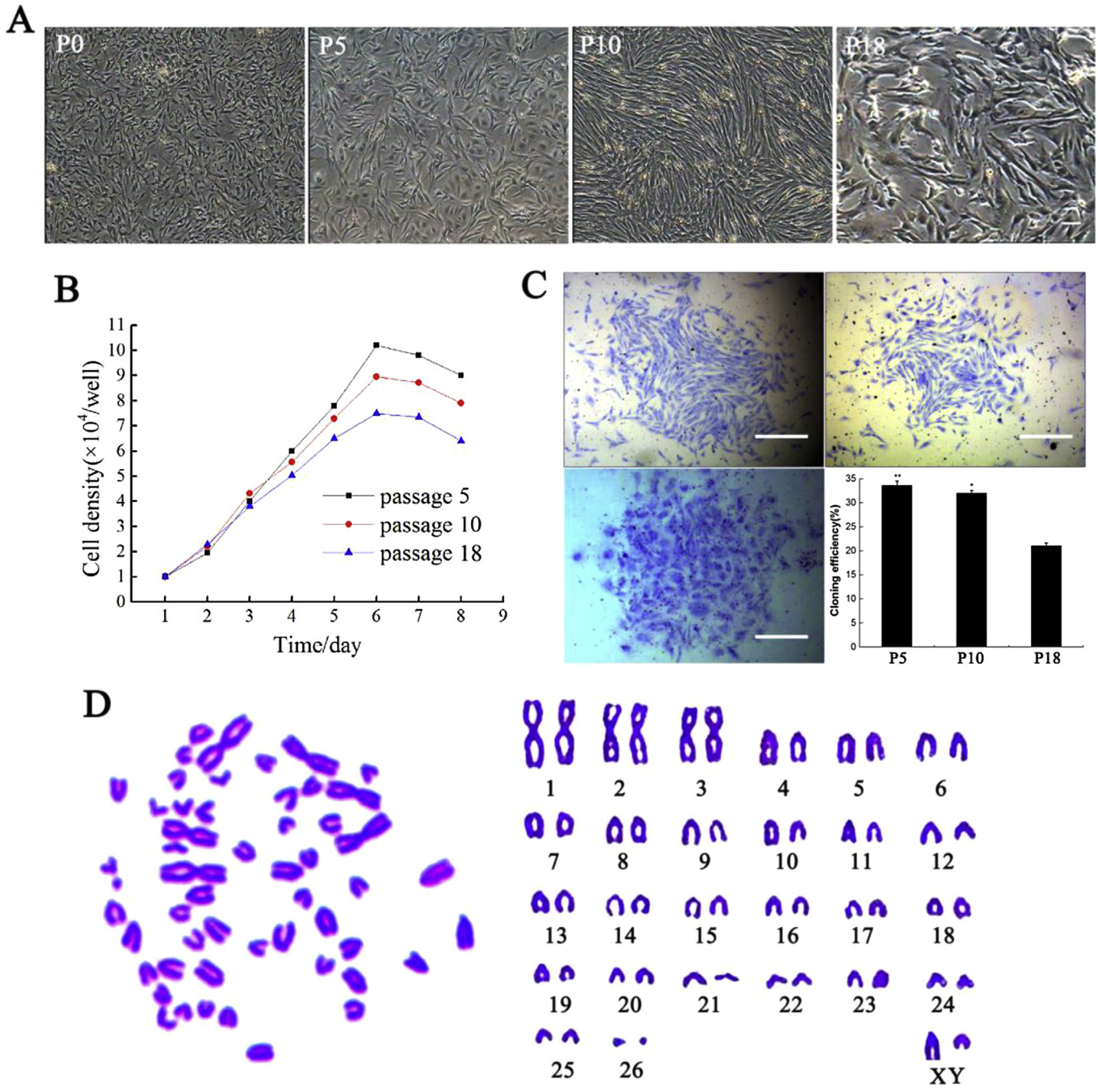

Fig. 1. Morphology, growth curves, colony forming and G-banding of L-MSCs in vitro. (A) Cell morphology analysis of primary and sub-cultured fetal sheep L-MSCs; (B) Growth curves of L-MSCs at P5, P10 and P18. Cell density reflected by the vertical axis. (C) Representative CFU derived from L-MSCs cultured for 1 week (scale bar equates to 200 μm). Bar chart shows that CFU number of different passages. (D) Chromosome G-banding of fetal sheep L-MSCs. Chromosomes at metaphase (left) and karyotype (right).

3.2. Growth kinetics, cell proliferation and cell apoptosis assays

The growth curves of the L-MSCs were all typically sigmoidal (Fig. 1B). These cells had similar proliferative potential, and PDTs were between 42.7 and 56.5 h. L-MSCs have greater CFU potential, and the colony-forming rates were 33.61 ± 0.89, 32.01 ± 0.55 and 21.01 ± 0.63colonies/100 cells, respectively (Fig. 1C). Cell cycle analysis showed that the majority of cells of P5, P10, P18 were in the G0/G1 phase (70.5–91.2%), indicating that most cells were consistent with quiescent property of stem cells. However, there are significant differences were identified about cell proportion of different cell phases among P5, P10, P18 (Fig. 2A). Although cell proliferation was significantly inhibited in P18 by BrdU indirect immunofluorescence (Fig. 2C), there were no obvious difference about rates of cell apoptosis and death among different passages (2.7%/P5, 3.3%/P10 and 6.6%/P18, $P > 0.05$, Fig. 2B).

3.3. Immunofluorescence characterization of stem cell markers in L-MSCs

The L-MSCs of fetal sheep could express surface antigens (CD29, CD44, CD71, CD73 and CD90), but hematopoietic cell markers CD34 and CD45 were negative, which was in accordance with human fetal L-MSCs (Fig. 3A). Moreover, the majority of L-MSCs (above 90%) could express the above-mentioned surface antigen markers in the viable cell population (Fig. 3C). And, qRT-PCR demonstrated that the L-MSCs could express pluripotent marker genes Oct4, Nanog and mesenchymal marker genes β-integrin, CD44, CD71, CD73 and CD90, but CD34 and CD45 were still not detected, which was identical with the immunofluorescence results above (Fig. 3B).

Differentiation of L-MSCs to Adipocytes, Osteoblasts, and Chondrocytes in vitro L-MSCs showed significant morphological changes from fibroblast-like to oblate with numerous intracellular lipid droplets or lipid vesicles under adipogenic induction (AID) conditions for 7 days (Fig. 4A). Adipogenic differentiation of L-MSCs was evidenced by positive Oil Red O staining and the expression of two adipocyte specific markers, PPARγ and LPL (Fig. 4B). After induction with osteoblast induction (OID) conditions for 14days, L-MSCs became aggregated and formed calcium deposits nodules, which were confirmed by Alizarin Red staining (Fig. 4C). And, the expression of osteogenic specific genes Coll I and OPN were significant increased (Fig. 4D). Histologically, under chondrocyte induction (CID) conditions for 14 days, chondrogenic differentiation of L-MSCs was confirmed by Alcian Blue staining and Toluidine Blue staining (Fig. 4E). Expression levels of the chondrocyte-specific genes Sox9, Coll II and CoX II were detected by RT-PCR. (Fig. 4 F).

3.4. Differentiation potential of L-MSCs toward β-cell, hepatocytes and neural cells

The islet-like clusters were stained with DTZ fluid and stained scarlet after induction over 10 days (Fig. 5A). Specific markers of pancreatic β-cells (PDX1 and insulin) were detected through immunofluorescence and RT-PCR (Fig. 5A, B). Glucose-induced insulin secretion *in vitro* was used to evaluate the functionality of pancreatic β-like cells. Insulin secretion was dose-dependent after

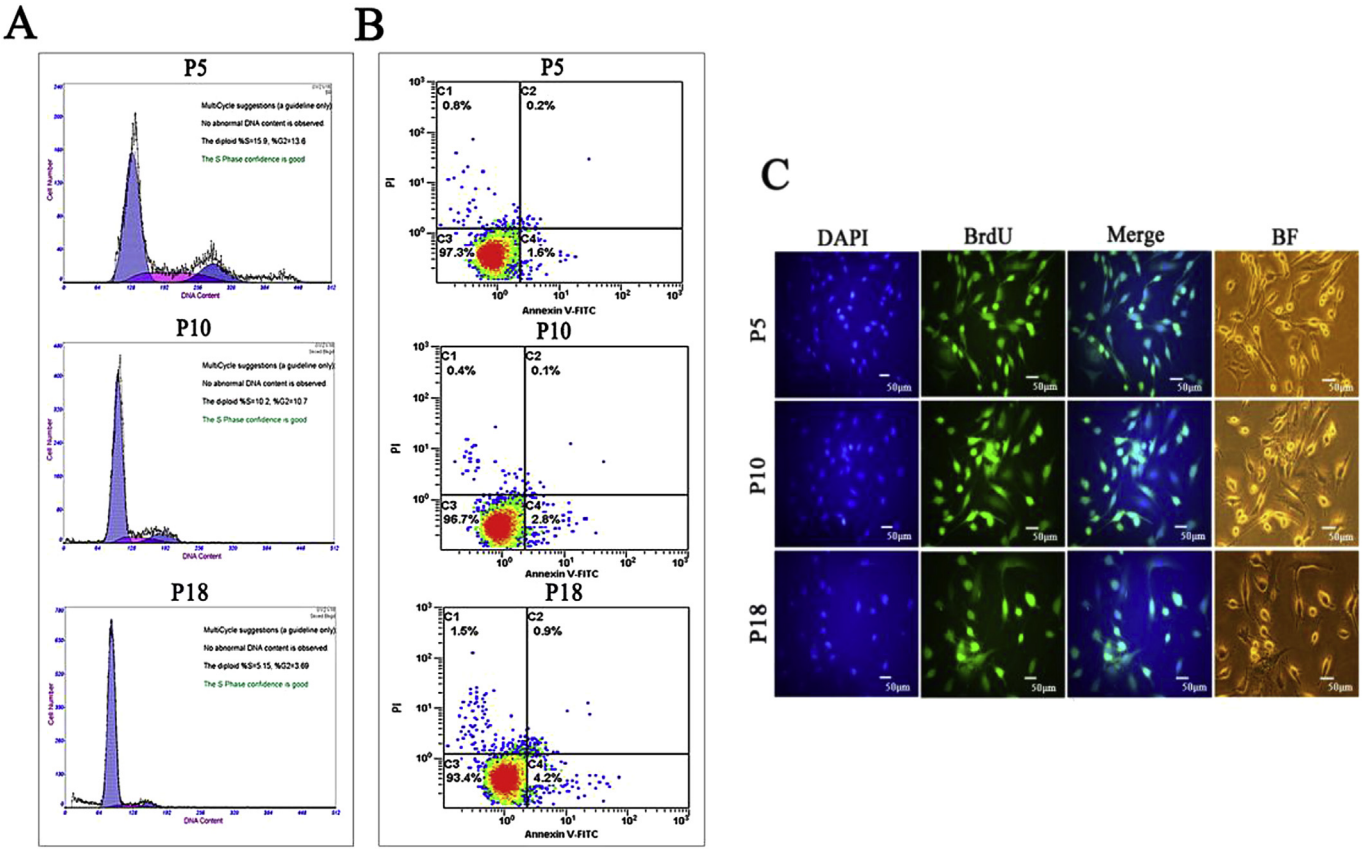

Fig. 2. Cell proliferation and cell apoptosis analysis of L-MSCs. (A) Flow cytometric analysis showed that the majority of L-MSCs of P5, P10, P18 were in the G0/G1 phase (70.5–91.2%); (B) Apoptotic rates of L-MSCs at P5, P10 and P18 were detected using AnnexinV-FITC/PI by flow cytometry (2.7–6.6%), and there were no significant difference among different passages (P > 0.05). (C) Immunodetection for BrdU incorporation of L-MSCs.

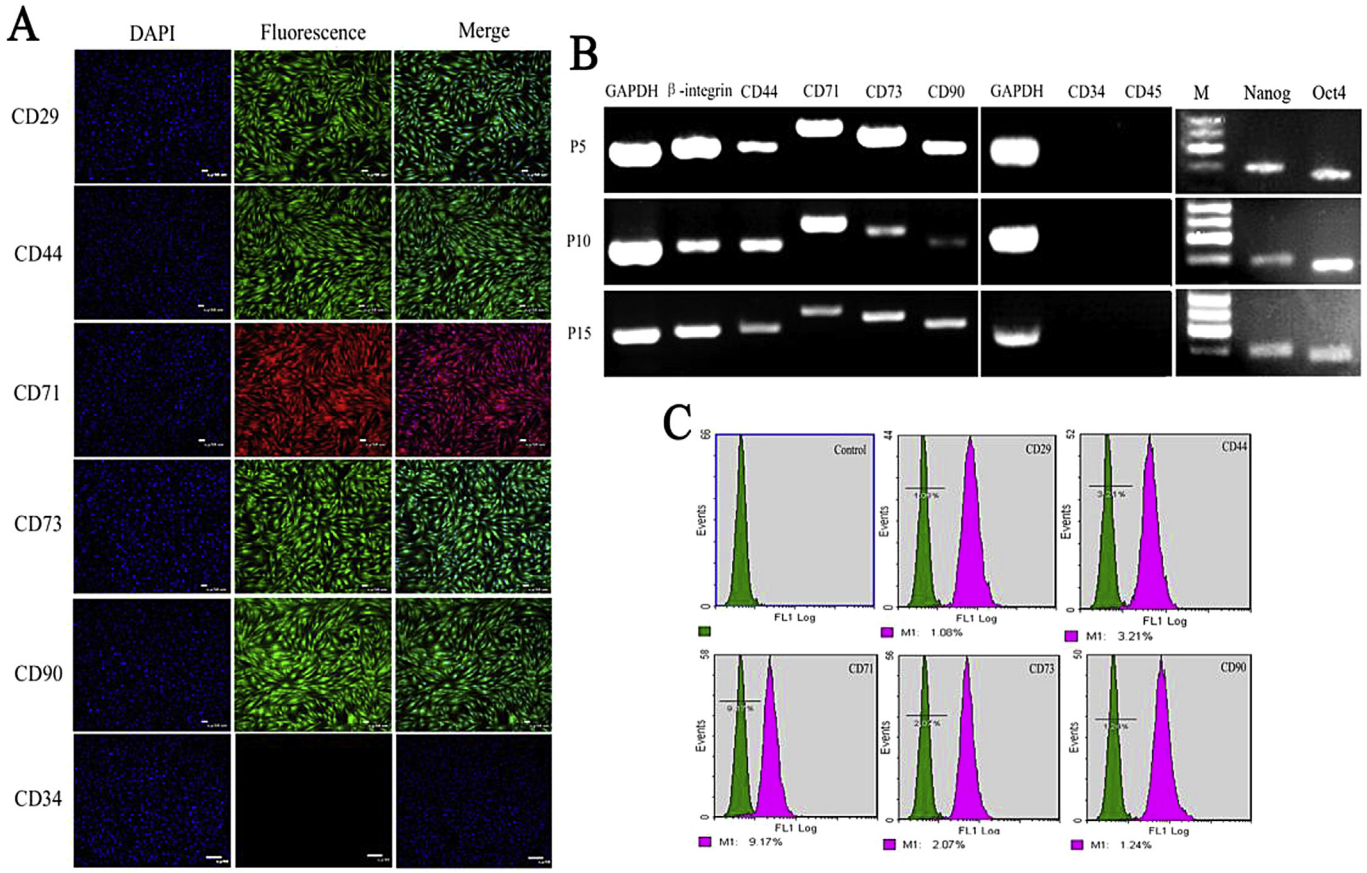

Fig. 3. Expression of Pluripotent and Mesenchymal Stem cell specific markers in L-MSCs. (A) Immunofluorescence stain showed the expression of mesenchymal stem cell markers (100 ×), DAPI, Blue; Scale bar = 50 μm; (B) The L-MSCs could express pluripotent marker genes Oct4, Nanog and mesenchymal marker genes by RT-PCR analysis. (C) The positive rate of surface antigens of L-MSCs was all above 90% analyzed by flow cytometry after colabeled, correspond to BMSCs.

incubation for 1 h with glucose (5.5 mM and 25.5 mM) (Fig. 5C). However, the total quantity of insulin produced was in the low range expressed, and flow cytometry further suggested only 37.62 ± 1.26% L-MSCs were possibly differentiated into insulin-secreting cells.

After 14 days of culture with hepatogenic inducing (HID) medium, spindle-shaped cells transformed into heterogeneous population of epithelial cells, then exhibited polygonal shape and mature hepatocyte-like morphology. Moreover, glycogen uptake was detected and most cells were positive by Periodic Acid-Schiff (PAS) staining (Fig. 5A). The expression of hepatogenic marker genes albumin (ALB) and α-fetoprotein (AFP) were significantly increased, determined by RT-PCR (Fig. 5B). Detoxification of ammonia into urea and its secretion are the main duties of hepatocytes. The levels of urea and ALB protein were significantly increased in a time-dependent manner as compared with negative control ($p < 0.01$, Fig. 5G).

Under neural-inducing (NID) condition for 14 days, L-MSCs demonstrated typically elongated cell bodies with multipolar and stellate morphology, grew with many branches and long axon of neurons. The expression of neural cell markers was evidenced by immunofluorescence, and MAP-2, NFM, Nestin were all positive (Fig. 5C). Furthermore, the expression of neural markers Map-2 and NF genes was also confirmed by RT-PCR (Fig. 5D), and the result demonstrated the differentiation potential of the L-MSCs to neurocytes.

4. Discussion

A high proliferation potential and multi-lineage differentiation capacity make MSCs a promising tool for regenerative medicine and tissue engineering as well as gene therapy. Recently, studies have demonstrated the profound therapeutic potential of L-MSCs for tissue homeostasis, restoration and regeneration of lung tissue in some animal model cell-transplantation assays [9,18]. And, recent studies suggested that fetal stem cells represent a more valuable and fascinating source of multipotent stem cells than adult stem cells [13]. However, L-MSCs from sheep lung and their localization in situ have not yet been reported.

Notably, we have successfully isolated L-MSCs populations from the lung tissues of 45-day-old embryonic sheep, and also attempted to unravel their fundamental differentiation potential *in vitro*. The fetal sheep L-MSCs were isolated using collagenase digestion, and could be substantially passaged for at least 18 passages *in vitro*. The colony-forming ability is essential for the self-renewal and specific differentiation characteristics of stem cells. The colony-forming efficiency of L-MSCs was between 21.01 and 33.61% at passages 5, 10 and 18, which showed there was no significant difference in the incidence of adherent clonogenic CFU-Fs between L-MSC and BMSCs. In comparison to other mammal-derived L-MSCs, fetal sheep L-MSCs exhibited preferable proliferation ability in culture process. In addition, we have demonstrated that L-MSCs could express a similar MSC-associated surface marker profile

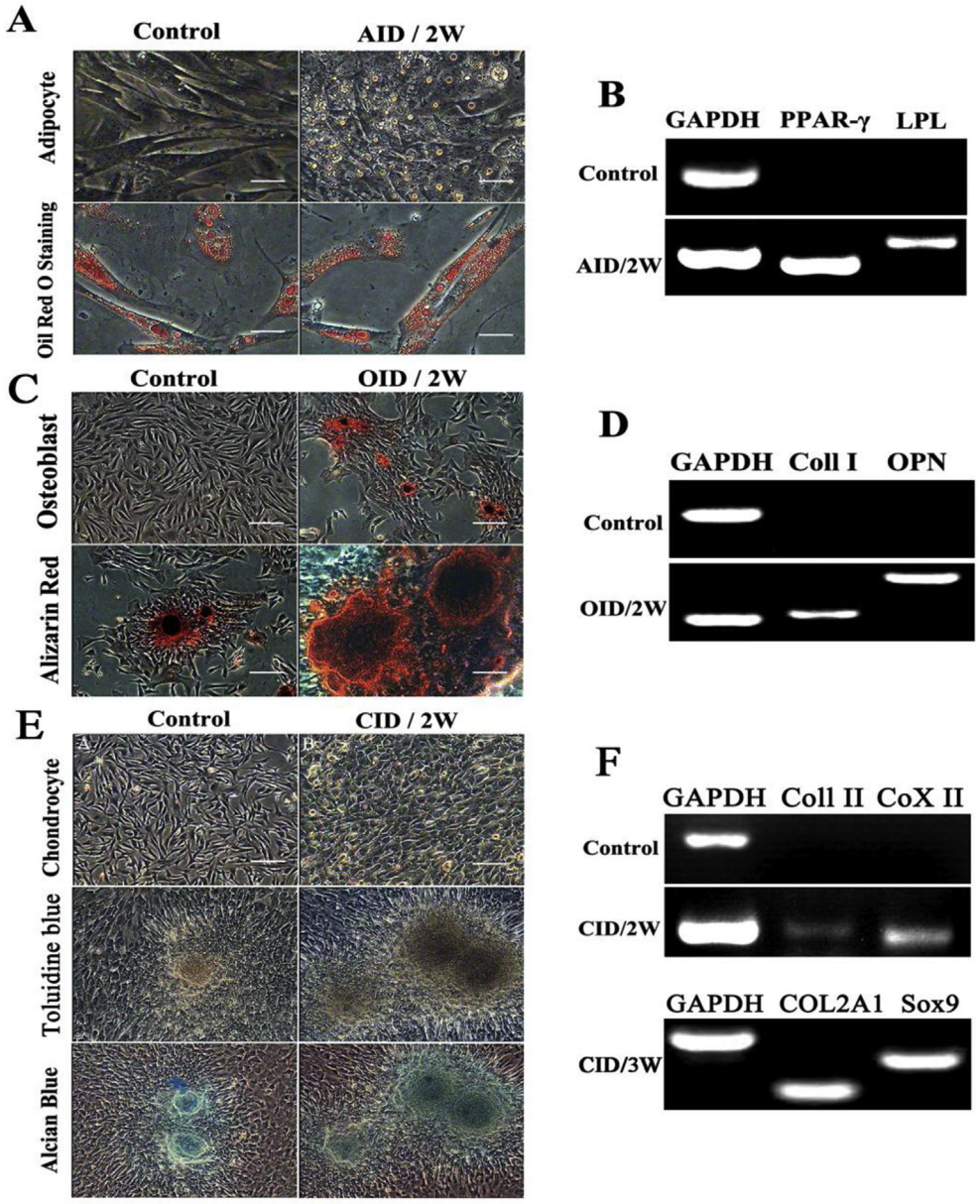

Fig. 4. Adipocyte, osteoblast and chondrocyte differentiation of L-MSCs. (A) Lipid droplets appeared in cytoplasm and were positive for Oil Red staining (40 × , 100 ×); (B) Gene-expression of adipocyte specific genes PPAR-γ and LPL were analyzed; (C) Calcium deposits were positive for alizarin red staining. (D) Expression of osteoblast specific markers OPN and Coll I were analyzed; (E) Chondrocyte differentiation was confirmed by Toluidine Blue and Alcian Blue staining; (F) Expression of chondrocyte-specific gene Coll II and Cox were detected by RT-PCR.

compared with BMSCs, including positivity for β-integrin, CD29, CD44, CD71, CD73 and CD90, and hematopoietic progenitor, leukocyte and monocyte/macrophage markers CD34 and CD45 were negative [9].

MSCs were an appealing multipotent candidate cell for cell therapies because of their multi-lineage differentiation [15]. We have demonstrated the L-MSCs cells exhibit a similar phenotypic profile and differentiation potential to BMSCs cells *in vitro*. Similarly, the fetal sheep L-MSCs can be induced to differentiate not only into mesoblastic cells such as adipocytes, osteoblasts and chondrocytes *in vitro*, but also cells of non-mesenchymal origin, such as β-cell, hepatocyte-like cells and neurogenic cells. Furthermore, the differentiation potential of L-MSCs was further supported by significantly upregulated mRNA expression levels of OPN, LPL, PPAR-γ (mesoderm), AFP and ALB (endoderm), and MAP2, NF(ectoderm) following induction in appropriate media for 4 weeks. It's worth mentioning that urea and ALB secretion by differentiated hepatocytes maintained the detoxification function. And, glucose-induced insulin secretion *in vitro* evaluated the functionality of pancreatic β-like cells, which demonstrated the differentiated cells maintained the similar function to cells *in vivo*. These results suggested that the L-MSCs posses the multi-lineage differentiations potential and can serve as desirable cell types for lung injury regeneration.

In the current study, the results evidenced that different inducing mediators could determine the differentiated direction of the L-MSCs. When out of range of 10^{-8} -10^{-10} moL/l, dexamethasone could inhibit the differentiation of fetal sheep L-MSCs into

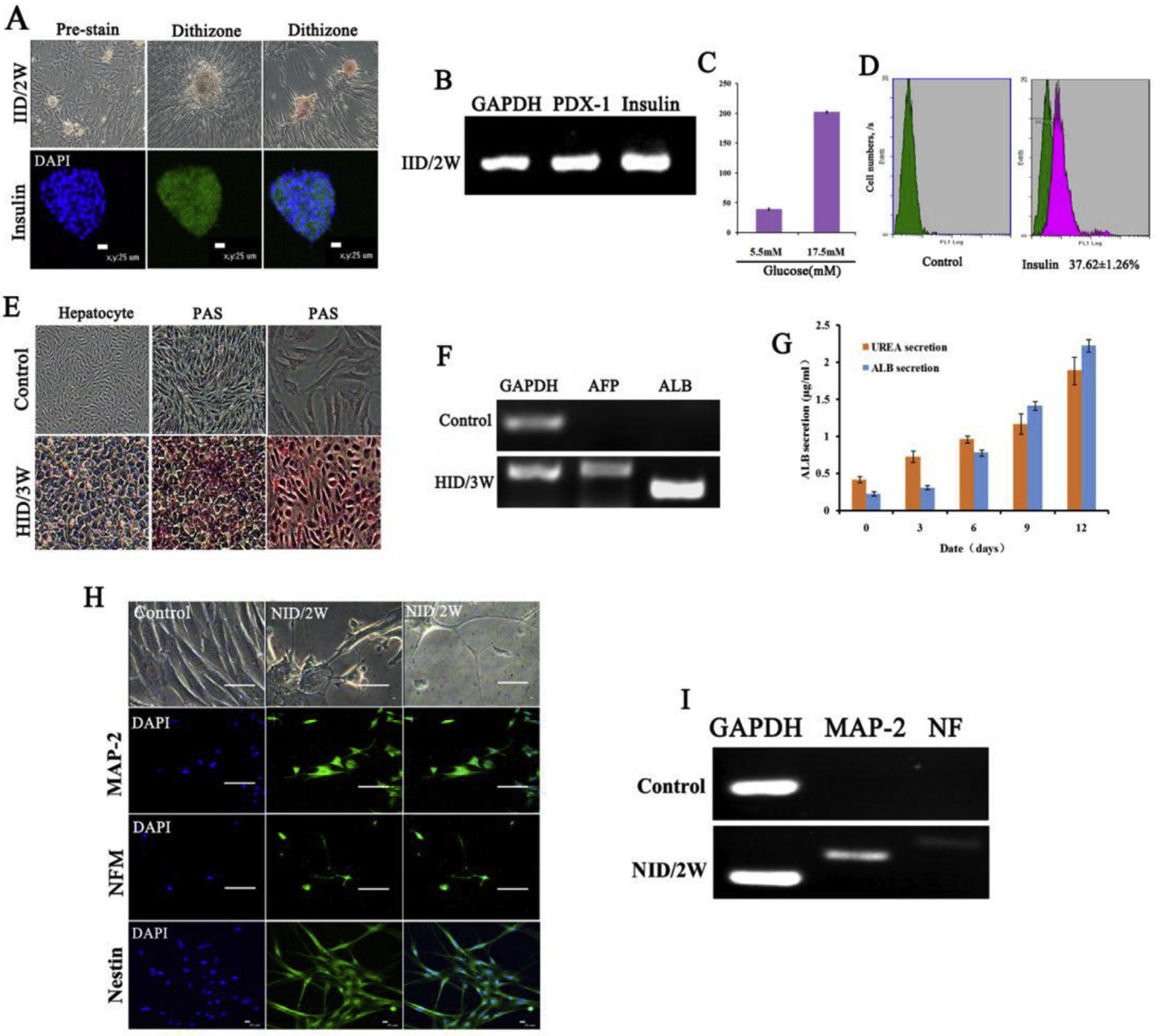

Fig. 5. β-cell, Hepatocytes and Neurocyte differentiation of L-MSCs. (A) The islet-like clusters were stained scarlet with DTZ fluid and immunofluorescence stain for insulin; (B) Expression of PDX1 and insulin were examined; (C) Glucose-induced insulin secretion(mean ± SEM) *in vitro* by ELISA test; (D) Only 37.62 ± 1.26% L-MSCs were differentiated into insulin-secreting cells; (E) The hepatogenic differentiated cells were positive by PAS assay; (F) Expression of hepatogenic cells marker genes ALB and AFB were analyzed; (G) The production of urea and albumin were significantly increased in a time-dependent manner ($p < 0.01$); (H) Expression of MAP2, NFM and Nestin was analyzed by immunofluorescence stain; (I) Expression of neuronal marker genes (MAP2, NF) was increased by RT-PCR analysis.

osteoblasts. Which in turn, dexamethasone might promote L-MSCs to differentiate into lipocytes at a higher concentration. Although neurotrophic factors GDNF, EGF or chemical inducers β-mercaptoethanol and DMSO, both could induce L-MSCs to differentiate into nerve cells, some researchers found that chemical inducers had negative effects on viability and morphological changes of MSCs in the process of induction [17]. Whereas GDNF significantly improved the viability of MSCs, and therefore was used for neurogenic differentiation [23]. The multilineage differentiation of L-MSCs together with their homotransplantation, immunosuppressive characteristics, demonstrate that these cells are promising alternative cell source for cell-based therapies and tissue engineering. However, there are still many drawbacks for these cells in cell therapies *in vivo*. More researches about differentiation mechanisms may be taken into account in future research, which will promote the use of L-MSCs in regenerative medicine.

Acknowledgments

This research was supported by the Agricultural Science and Technology Innovation Program (cxgc-ias-01), the National Natural Science Foundation of China (81301333, 31472064), the Natural Science Foundation of Anhui Province (1408085QH155), Key projects for outstanding young talent of Anhui Province (gxyqZD2016164).

Appendix A. Supplementary data

Supplementary data related to this article can be found at http://dx.doi.org/10.1016/j.cryobiol.2017.03.003.

References

[1] T. Asari, K. Furukawa, S. Tanaka, H. Kudo, H. Mizukami, A. Ono, T. Numasawa, G. Kumagai, S. Motomura, S. Yagihashi, S. Toh, Mesenchymal stem cell isolation and characterization from human spinal ligaments, Biochem. biophysical Res. Commun. 417 (2012) 1193–1199.

[2] A. Bernhardt, A. Lode, F. Peters, M. Gelinsky, Optimization of culture conditions for osteogenically-induced mesenchymal stem cells in beta-tricalcium phosphate ceramics with large interconnected channels, J. tissue Eng. Regen. Med. 5 (2011) 444–453.

[3] B. Blum, N. Benvenisty, The tumorigenicity of diploid and aneuploid human pluripotent stem cells, Cell Cycle 8 (2009) 3822–3830.

[4] A.D. Cohen, M.J. Zigmond, A.D. Smith, Effects of intrastriatal GDNF on the response of dopamine neurons to 6-hydroxydopamine: time course of protection and neurorestoration, Brain Res. 1370 (2011) 80–88.

[5] W.L. Corwin, J.M. Baust, J.G. Baust, R.G. Van Buskirk, Characterization and modulation of human mesenchymal stem cell stress pathway response following hypothermic storage, Cryobiology 68 (2014) 215–226.

[6] M. Dominici, K. Le Blanc, I. Mueller, I. Slaper-Cortenbach, F. Marini, D. Krause, R. Deans, A. Keating, D. Prockop, E. Horwitz, Minimal criteria for defining multipotent mesenchymal stromal cells. The International Society for Cellular Therapy position statement, Cytotherapy 8 (2006) 315–317.

[7] M.L. Gonzalez-Fernandez, S. Perez-Castrillo, P. Ordas-Fernandez, M.E. Lopez-Gonzalez, B. Colaco, V. Villar-Suarez, Study on viability and chondrogenic differentiation of cryopreserved adipose tissue-derived mesenchymal stromal cells for future use in regenerative medicine, Cryobiology 71 (2015) 256–263.

[8] Q. Hao, Y.G. Zhu, A. Monsel, S. Gennai, T. Lee, F. Xu, J.W. Lee, Study of bone marrow and embryonic stem cell-derived human mesenchymal stem cells for treatment of Escherichia coli endotoxin-induced acute lung injury in mice, Stem cells Transl. Med. 4 (2015) 832–840.

[9] J. Kajstura, M. Rota, S.R. Hall, T. Hosoda, D. D'Amario, F. Sanada, H. Zheng, B. Ogorek, C. Rondon-Clavo, J. Ferreira-Martins, A. Matsuda, C. Arranto, P. Goichberg, G. Giordano, K.J. Haley, S. Bardelli, H. Rayatzadeh, X. Liu, F. Quaini, R. Liao, A. Leri, M.A. Perrella, J. Loscalzo, P. Anversa, Evidence for human lung stem cells, The. New Engl. J. Med. 364 (2011) 1795–1806.

[10] S. Kumar, M. Vaidya, Hypoxia inhibits mesenchymal stem cell proliferation through HIF1alpha-dependent regulation of P27, Mol. Cell. Biochem. 415 (2016) 29–38.

[11] X. Li, Y. Guo, Y. Yao, J. Hua, Y. Ma, C. Liu, W. Guan, Reversine increases the plasticity of long-term cryopreserved fibroblasts to multipotent progenitor cells through activation of Oct4, Int. J. Biol. Sci. 12 (2016) 53–62.

[12] L. Ling, Y. Ni, Q. Wang, H. Wang, S. Hao, Y. Hu, W. Jiang, Y. Hou, Trans-differentiation of mesenchymal stem cells derived from human fetal lung to hepatocyte-like cells, Cell Biol. Int. 32 (2008) 1091–1098.

[13] K.L. Lye, N. Nordin, S. Vidyadaran, K. Thilakavathy, Mesenchymal stem cells: From stem cells to sarcomas, Cell Biol. Int. 40 (2016) 610–618.

[14] C. Ma, Y. Guo, H. Liu, K. Wang, J. Yang, X. Li, C. Liu, W. Guan, Isolation and biological characterization of a novel type of pulmonary mesenchymal stem cells derived from Wuzhishan miniature pig embryo, Cell Biol. Int. 40 (2016) 1041–1049.

[15] L.A. Ortiz, F. Gambelli, C. McBride, D. Gaupp, M. Baddoo, N. Kaminski, D.G. Phinney, Mesenchymal stem cell engraftment in lung is enhanced in response to bleomycin exposure and ameliorates its fibrotic effects, Proc. Natl. Acad. Sci. United States of America 100 (2003) 8407–8411.

[16] M. Ricciardi, G. Malpeli, F. Bifari, G. Bassi, L. Pacelli, A.H. Nwabo Kamdje, M. Chilosi, M. Krampera, Comparison of epithelial differentiation and immune regulatory properties of mesenchymal stromal cells derived from human lung and bone marrow, PloS one 7 (2012) e35639.

[17] J. Sagara, N. Makino, Glutathione induces neuronal differentiation in rat bone marrow stromal cells, Neurochem. Res. 33 (2008) 16–21.

[18] H.K. Salem, C. Thiemermann, Mesenchymal stromal cells: current understanding and clinical status, Stem Cells 28 (2010) 585–596.

[19] K. Sinclair, S.T. Yerkovich, D.C. Chambers, Mesenchymal stem cells and the lung, Respirology 18 (2013) 397–411.

[20] R.B. Subbarao, I. Ullah, E.J. Kim, S.J. Jang, W.J. Lee, R.H. Jeon, D. Kang, S.L. Lee, B.W. Park, G.J. Rho, Characterization and evaluation of neuronal trans-differentiation with electrophysiological properties of mesenchymal stem cells isolated from porcine endometrium, Int. J. Mol. Sci. 16 (2015) 10934–10951.

[21] M. Wang, G. Zhang, Y. Wang, T. Liu, Y. Zhang, Y. An, Y. Li, Crosstalk of mesenchymal stem cells and macrophages promotes cardiac muscle repair, Int. J. Biochem. cell Biol. 58 (2015a) 53–61.

[22] S. Wang, L. Guo, J. Ge, L. Yu, T. Cai, R. Tian, Y. Jiang, R.C. Zhao, Y. Wu, Excess integrins cause lung entrapment of mesenchymal stem cells, Stem Cells (2015b).

[23] J.D. Yang, H. Cheng, J.C. Wang, X.M. Feng, Y.N. Li, H.X. Xiao, The isolation and cultivation of bone marrow stem cells and evaluation of differences for neural-like cells differentiation under the induction with neurotrophic factors, Cytotechnology 66 (2014) 1007–1019.